

International Journal of Modern Physics E  
 © World Scientific Publishing Company

## Universal descriptions of chemical freeze-out based on pressure and specific heat respectively

Subhasis Samanta <sup>1 2</sup>

<sup>1</sup>*School of Physical Sciences, National Institute of Science Education and Research, HBNI,  
 Jatni - 752050, India  
 subhasis.samant@gmail.com*

<sup>2</sup>*Center for Astroparticle Physics & Space Science, Bose Institute, Block-EN, Sector-V, Salt  
 Lake, Kolkata-700091, India  
 &  
 Department of Physics, Bose Institute,  
 93/1, A. P. C Road, Kolkata - 700009, India*

Received Day Month Year

Revised Day Month Year

The lattice QCD data of pressure and the energy density have been used to extract the hadronic radius parameter of the excluded volume hadron resonance gas (EVHRG) model. The equation of state can be described well with the extracted radius parameter  $R_h = 0.15$  fm. Specific heat is also calculated in the EVHRG model. Further, two new universal descriptions of chemical freeze-out parameters have been introduced based on pressure and specific heat respectively. It is shown that the chemical freeze-out parameters obtained at various  $\sqrt{s_{NN}}$  in ideal HRG model approximately correspond to  $P/T^4 = 0.88$  and  $C_V/T^3 = 47$  respectively. These two quantities are important to describe the thermodynamic properties of the hadronic matter created in heavy ion collision experiment. The sensitivity of universal chemical freeze-out lines on repulsive interaction is also studied. It has been observed that the behaviors of chemical freeze-out lines for  $P/T^4$  and  $C_V/T^3$  in EVHRG model remain similar to ideal HRG model for the best fit value of hadronic radii.

*Keywords:* Heavy Ion collision; Hadron Resonance Gas model; Chemical Freeze-out.

PACS numbers: 25.75.-q; 24.10.Pa

### 1. Introduction

In the last few years, a substantial amount of experimental and theoretical efforts have been devoted worldwide to investigate the strongly interacting matter under extreme conditions of temperature and/or baryon chemical potential. While at low baryon chemical potential and high temperature lattice quantum chromo dynamics (LQCD) data seem to indicate a smooth crossover from hadronic to quark-gluon plasma (QGP) phase,<sup>1</sup> at high baryon chemical potential and low temperature the system is expected to have a first-order phase transition.<sup>2</sup> This first order phase

transition line at high baryon chemical potential and low temperature should end at a critical end point (CEP), a second-order phase transition point as one moves towards the high temperature and low baryon chemical potential region, in the QCD phase diagram. Heavy ion collisions provide a unique tool to create and study strongly interacting matter under extreme conditions of temperature and/or baryon chemical potential. One of the primary goals of heavy-ion collision experiments is to map QCD phase diagram in terms of temperature and baryon chemical potential. At present, the properties of QCD matter at high temperature and almost zero baryon chemical potential are being investigated using ultra relativistic heavy ion collisions at the Large Hadron Collider (LHC), CERN and Relativistic Heavy Ion Collider (RHIC), Brookhaven National Laboratory (BNL). The Beam Energy Scan (BES) program of RHIC is currently investigating the location of the CEP. The HADES experiment at GSI, Darmstadt is investigating medium of very large baryon chemical potential. The region of large baryon chemical potential will also be explored by the NA61-SHINE experiment at CERN-SPS. In future, the Compressed Baryonic Matter (CBM) experiment at the Facility for Antiproton and Ion Research (FAIR) at GSI and the Nuclotron-based Ion Collider fAcility (NICA) at JINR, Dubna will also study nuclear matter at large baryon chemical potential.

LQCD provides the most direct approach to study the QCD matter at high temperature. However, at finite chemical potential, LQCD faces the well-known sign problem. On the other hand, the hadron resonance gas (HRG) model<sup>3–34</sup> which is used in this present work, provide a simpler alternative to study strongly interacting matter at finite temperature and chemical potential. The HRG model is quite successful in describing the bulk properties of hadronic matter in thermal and chemical equilibrium<sup>13,14,19</sup>. This model is also successful in describing the ratios of hadron yields, at chemical freeze-out, created in central heavy ion collisions from SIS up to RHIC energies<sup>6,7,9–11,15–17</sup>. In a heavy ion collision experiment, the chemical freeze-out is defined as the stage in the evolution of the thermal system when inelastic collisions among the hadrons cease and the hadronic ratios become fixed. At various center-of-mass energies  $\sqrt{s_{NN}}$ , hadronic yields or ratios are generally analyzed phenomenologically using HRG model<sup>15,16,35–39</sup> to determine the chemical freeze-out parameters. Relations of chemical freeze-out temperature and baryon chemical potential with  $\sqrt{s_{NN}}$  establish the chemical freeze-out line<sup>16,35</sup> in the QCD phase diagram. The main result of these investigations is that the chemical freeze-out temperature increases sharply from SIS up to SPS energies and reaches, for higher collision energies, at constant values near  $T = 160 - 165$  MeV while baryon chemical potential decreases sharply as a function of  $\sqrt{s_{NN}}$ . Chemical freeze-out is the earliest stage in the evolution of the hadronic phase which can be determined phenomenologically from the experiment data. Therefore, the chemical freeze-out line is very much important in the QCD phase diagram. To know the thermodynamic properties of the system at chemical freeze-out we have to study equation of state of the matter. There are several universal chemical freeze-out descriptions in the existing literature which can approximately describe the chemical

freeze-out line in the QCD phase diagram. Those universal properties will be discussed in detail in this paper. Those universal chemical freeze-out descriptions are independent of  $\sqrt{s_{NN}}$  and they are related to the equation of state of the thermal system. Those universal properties will be useful to study properties of thermal system created in heavy-ion collisions at any  $\sqrt{s_{NN}}$ . Finding out the universal conditions of chemical freeze-out parameters have been the subject of various studies.

The aim of the present work is twofold. First, I would like to study some basic bulk thermodynamic quantities, where all the hadrons in HRG model contribute, like pressure, energy density, entropy density and specific heat of the matter in the HRG and an EVHRG model. Second, I would like to find out universal conditions of chemical freeze-out descriptions from those thermodynamic quantities.

The paper is organized as follows. First, the ideal HRG model and an EVHRG model are briefly discussed in Sec. 2. The Sec. 3 shows results of this paper. In Sec. 3.1 the effect of repulsive interaction at zero chemical potential has been studied using the LQCD data of equation of state. Further, in Sec. 3.2 result of specific heat at  $\mu = 0$  has been shown. Thereafter, two new universal chemical freeze-out descriptions based on pressure and specific heat respectively have been proposed in the Sec. 3.3. Furthermore, the behavior of universal chemical freeze-out lines in presence of repulsive interaction has been studied in Sec. 4. Finally in the Sec. 5, I conclude the findings of the paper.

## 2. Hadron Resonance Gas model

In the HRG model, the thermal system consists of all the hadrons and resonances. There are varieties of HRG models in the existing literature. Different versions of this model and some of the recent works using these models may be found in Refs. 3–34, 40–45. The logarithm of the partition function of a hadron resonance gas in the grand canonical ensemble can be written as

$$\ln Z^{id} = \sum_i \ln Z_i^{id}, \quad (1)$$

where the sum is over all the hadrons and resonances, *id* refers to ideal *i.e.*, non-interacting HRG model. For hadron species *i*,

$$\ln Z_i^{id} = \pm \frac{V g_i}{2\pi^2} \int_0^\infty p^2 dp \ln[1 \pm \exp(-(E_i - \mu_i)/T)], \quad (2)$$

where *V* is the volume of the thermal system, *T* is the temperature, *g<sub>i</sub>* is the degeneracy factor, *m<sub>i</sub>* is the mass,  $E_i(p) = \sqrt{p^2 + m_i^2}$  is the single particle energy and  $\mu_i = B_i\mu_B + S_i\mu_S + Q_i\mu_Q$  is the chemical potential. In the last expression, *B<sub>i</sub>*, *S<sub>i</sub>*, *Q<sub>i</sub>* are respectively the baryon number, strangeness and electric charge of the hadron,  $\mu$ 's are corresponding chemical potentials. The upper and lower sign corresponds to baryons and mesons respectively. In this present work, all the hadrons and resonances listed in the particle data book up to a mass of 3 GeV<sup>46</sup> have been incorporated. The width of the resonances are taken as zero. In this approximation

a resonance behaves identically to that of a stable hadron.<sup>47</sup> Hence resonance decay is also not there in this model. It is assumed that the hadronic matter is in thermal and chemical equilibrium. The partition function is the basic quantity from which one can calculate various thermodynamic quantities of the thermal system. The pressure  $P^{id}$ , energy density  $\varepsilon^{id}$ , entropy density  $s^{id}$  and the number density  $n^{id}$  of the thermal system can be calculated using the standard definitions,

$$\begin{aligned} P^{id} &= \sum_i P_i^{id} = \sum_i T \frac{\partial \ln Z_i^{id}}{\partial V} \\ &= \sum_i \pm \frac{g_i T}{2\pi^2} \int_0^\infty p^2 dp \ln[1 \pm \exp(-(E_i - \mu_i)/T)], \end{aligned} \quad (3)$$

$$\begin{aligned} \varepsilon^{id} &= \sum_i \varepsilon_i^{id} = - \sum_i \frac{1}{V} \left( \frac{\partial \ln Z_i^{id}}{\partial \frac{1}{T}} \right)_{\mu} \\ &= \sum_i \frac{g_i}{2\pi^2} \int_0^\infty \frac{p^2 dp}{\exp[(E_i - \mu_i)/T] \pm 1} E_i, \end{aligned} \quad (4)$$

$$\begin{aligned} s^{id} &= \sum_i \frac{1}{V} \left( \frac{\partial (T \ln Z_i^{id})}{\partial T} \right)_{V, \mu} \\ &= \sum_i \pm \frac{g_i}{2\pi^2} \int_0^\infty p^2 dp \left[ \ln \left( 1 \pm \exp\left(-\frac{(E_i - \mu_i)}{T}\right) \right) \pm \frac{(E_i - \mu_i)}{T(\exp((E_i - \mu_i)/T) \pm 1)} \right]. \end{aligned} \quad (5)$$

$$\begin{aligned} n^{id} &= \sum_i \frac{T}{V} \left( \frac{\partial \ln Z_i^{id}}{\partial \mu_i} \right)_{V, T} \\ &= \sum_i \frac{g_i}{2\pi^2} \int_0^\infty \frac{p^2 dp}{\exp[(E_i - \mu_i)/T] \pm 1}. \end{aligned} \quad (6)$$

In case of heavy-ion collision experiments, the parameters  $T$  and  $\mu$ 's of HRG model corresponds to those at chemical freeze-out which are believed to depend on initial conditions of the collision due to global charge conservation. That means conserved initial charges of the system will not change even after the collision. The chemical potentials at chemical freeze-out  $\mu_B, \mu_S$  and  $\mu_Q$  are not independent but related (on average) to each other as well as to the  $T$  via the relations<sup>48</sup>

$$\sum_i n_i(T, \mu_B, \mu_S, \mu_Q) S_i = 0, \quad (7)$$

and

$$\sum_i n_i(T, \mu_B, \mu_S, \mu_Q) Q_i = r \sum_i n_i(T, \mu_B, \mu_S, \mu_Q) B_i, \quad (8)$$

where  $n_i$  is the number density of  $i$  th hadron at chemical freeze-out,  $r$  is the ratio of net-charge to net-baryon number of the colliding nuclei. For central Au + Au or Pb + Pb collisions  $r = N_p/(N_p + N_n) = 0.4$ , where  $N_p$  and  $N_n$  are respectively proton numbers and neutron numbers of the colliding nuclei. The right-hand side of the Eq. 7 is zero since initially there is no net-strangeness in the colliding nuclei. Similarly Eq. 8 is due to the conservation of electric charge and baryon number.

### 2.1. Excluded Volume Hadron Resonance Gas model

In the ideal HRG model hadrons and resonances are point-like. Although attractive interactions between hadrons are incorporated through the presence of resonances, repulsive interactions are ignored completely in this framework. However, the repulsive interactions are also needed, especially at very high temperature and/ or large baryonic chemical potential, to catch the basic qualitative features of strong interactions where the ideal gas assumption becomes inadequate. In the EVHRG model<sup>3-5, 8, 18, 19, 21, 22, 24, 26-29, 40-43, 45, 49-51</sup> hadronic phase is modeled by a gas of interacting hadrons, where the geometrical sizes of the hadrons are explicitly incorporated as the excluded volume correction to approximate the short-range van der Waals type repulsive interaction. Excluded volume corrections were first introduced in Ref.<sup>3</sup> but it was thermodynamically inconsistent. A thermodynamically consistent excluded volume correction was first proposed in Ref.<sup>4</sup>

In a thermodynamically consistent EVHRG model pressure can be written as<sup>4, 8, 19</sup>

$$P(T, \mu_1, \mu_2, \dots) = \sum_i P_i^{id}(T, \hat{\mu}_1, \hat{\mu}_2, \dots), \quad (9)$$

where for the  $i$ -th hadron the effective chemical potential is

$$\hat{\mu}_i = \mu_i - V_{ev,i} P(T, \mu_1, \mu_2, \dots) \quad (10)$$

where  $V_{ev,i} = 4 \frac{4}{3} \pi R_i^3$  is the volume excluded for that hadron with hardcore radius  $R_i$ . In an iterative procedure, one can get the pressure. In this work we consider same radii  $R_h$  for all the hadrons. The pressure  $P(T, \mu_1, \mu_2, \dots)$  is suppressed compared to the ideal gas pressure  $P^{id}$  because of the smaller value of effective chemical potential. The other thermodynamic quantities like  $\varepsilon$ ,  $s$  and  $n$  can be calculated from Eqs. 9 - 10 as

$$\varepsilon = \varepsilon(T, \mu_1, \mu_2, \dots) = \frac{\sum_i \varepsilon_i^{id}(T, \hat{\mu}_i)}{1 + \sum_k V_{ev,k} n_k^{id}(T, \hat{\mu}_k)}, \quad (11)$$

$$s = s(T, \mu_1, \mu_2, \dots) = \left( \frac{\partial P}{\partial T} \right)_{\mu_1, \mu_2, \dots} = \frac{\sum_i s_i^{id}(T, \hat{\mu}_i)}{1 + \sum_k V_{ev,k} n_k^{id}(T, \hat{\mu}_k)}, \quad (12)$$

$$n = \sum_i n_i(T, \mu_1, \mu_2, \dots) = \frac{\sum_i n_i^{id}(T, \hat{\mu}_i)}{1 + \sum_k V_{ev,k} n_k^{id}(T, \hat{\mu}_k)}. \quad (13)$$

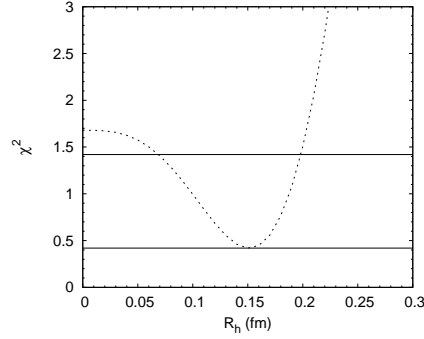


Fig. 1. The variation of  $\chi^2$  with the hardcore radii of hadrons ( $R_h$ ) at  $\mu = 0$ . LQCD data of  $^{53}$  have been used to calculate  $\chi^2$ . Horizontal lines in this plot correspond to the  $\chi^2_{min}$  and the  $\chi^2_{min} + 1$  values.

This EVHRG model is thermodynamically consistent *i.e.*, equation of state after excluded volume corrections obey the relation

$$\varepsilon + P - \sum_i \mu_i n_i = T s. \quad (14)$$

Recently, effects of excluded-volume have been studied in the equation of state of pure Yang-Mills theory.<sup>52</sup>

### 3. Results

#### 3.1. Equations of state at $\mu = 0$

The difference of the EVHRG model, as compared to HRG, is governed by the radius parameter. In this work I have tried to estimate the value of hardcore radius parameter by fitting LQCD data of equation of state instead of tuning  $R_h$  by hand. Continuum limit LQCD data<sup>53</sup> of two independent thermodynamic observables of the equation of state namely normalized pressure and energy density calculated at  $\mu = 0$  have been used to understand the effect repulsive interaction in terms of hard core radii of hadrons in EVHRG model. Using those LQCD data,  $\chi^2$  has been calculated at different radii of hadrons  $R_h$  where  $\chi^2$  has been defined as

$$\chi^2 = \frac{1}{N} \sum_i \left[ \frac{\left( \left( \frac{P}{T^4} \right)_i^{LQCD} - \left( \frac{P}{T^4} \right)_i^{EVHRG}(R_h) \right)^2}{\left( \left( \Delta \frac{P}{T^4} \right)_i^{LQCD} \right)^2} + \frac{\left( \left( \frac{\varepsilon}{T^4} \right)_i^{LQCD} - \left( \frac{\varepsilon}{T^4} \right)_i^{EVHRG}(R_h) \right)^2}{\left( \left( \Delta \frac{\varepsilon}{T^4} \right)_i^{LQCD} \right)^2} \right]. \quad (15)$$

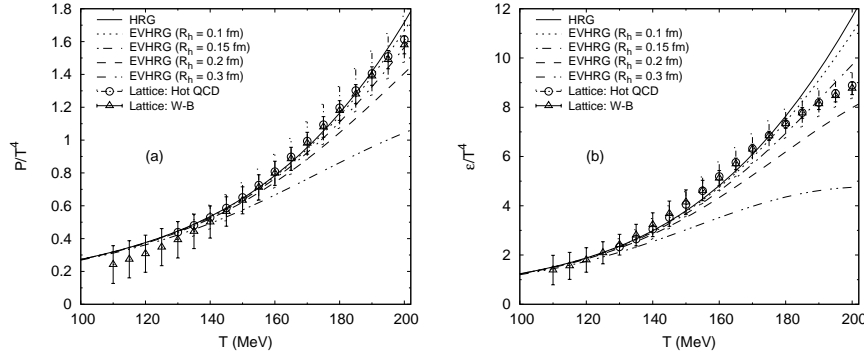


Fig. 2. Variation of normalized pressure (a) and energy density (b) with the temperature at  $\mu = 0$ . Continuum limit lattice QCD data are taken from Hot QCD Collaboration<sup>53</sup> and Wuppertal-Budapest Collaboration.<sup>54</sup>

In the last expression,  $(\Delta \frac{P}{T})_i^{LQCD}$  and  $(\Delta \frac{\epsilon}{T})_i^{LQCD}$  are the errors of normalized pressure and energy density respectively at the  $i$  th point calculated in the LQCD and  $N$  is the number of LQCD data points.

Figure 1 shows the variation of the  $\chi^2$  with hardcore radius parameter of hadrons  $R_h$ . Same radii for all the mesons and baryons have been considered in this work. The upper limit of temperature for the continuum limit LQCD data<sup>53</sup> is taken as  $T = 200$  MeV to calculate  $\chi^2$  of Fig. 1. It has been assumed that below  $T = 200$  MeV HRG and EVHRG models are valid to describe thermodynamic quantities because for this temperature equation states for both ideal HRG and EVHRG are well below the Stefan-Boltzmann limit for the deconfined QGP phase. Horizontal lines in the Fig. 1 indicate the  $\chi_{min}^2$  and the  $\chi_{min}^2 + 1$  values. The  $\chi_{min}^2$  corresponds to the best fit of the LQCD data and the  $\chi_{min}^2 + 1$  indicate the errors<sup>16,51</sup> on the parameter  $R_h$ . One can see from the Fig. 1, the best fit in terms of  $\chi^2$  is achieved at  $R_h = 0.15^{+0.04}_{-0.08}$  fm with  $\chi_{min}^2 = 0.42$ . This estimate is slightly smaller compared to the previous observations<sup>19,24</sup> where it was shown that most of the thermodynamic quantities can be described taking hadronic radii between  $0.2 - 0.3$  fm. The value of the hardcore radius was estimated as  $R_h = 0.3$  fm in the Ref.<sup>9</sup> Whereas in Ref.<sup>8</sup>  $R_h = 0.3 - 0.8$  fm was used to fit experimental hadronic yields. Although this estimation of  $R_h$  in this present work depends on the range of temperature used for the fit it will give us some idea about the  $R_h$  of EVHRG model where only one extra parameter ( $R_h$ ) is introduced compared to the ideal HRG model.

Figure 2 shows the temperature dependence of normalized pressure and normalized energy density respectively at  $\mu = 0$ . Results of ideal HRG model have been represented by solid lines. Other lines correspond to the results of the interacting HRG model or the EVHRG model with different radii of hadrons ( $R_h$ ). It can be seen that there is almost no effect of interaction till  $T \simeq 120$  MeV both

in pressure and energy density. The reason for this is that the effective degree of freedom of the system does not increase much up to this temperature and therefore correction due to excluded volume is small. Beyond  $T = 120$  MeV a substantial change in these quantities has been observed. It can be seen from this figure that at large  $T$  normalized pressure as well as normalized energy density are suppressed compared to the ideal HRG if we take non-zero hardcore radii of the hadrons. This is expected since hadrons start interacting at large temperature where the hadronic population is large. Further, suppression increases with the increase of radii of the hadrons. The continuum limit LQCD data of Hot QCD Collaboration<sup>53</sup> and Wuppertal-Budapest Collaboration<sup>54</sup> have also been plotted in this figure. Figure 2(a) illustrates the excellent agreement between the ideal HRG and the lattice QCD calculations of normalized pressure. On the other hand, one can see from Fig. 2(b) that normalized energy density calculated in ideal HRG model is close to the LQCD data up to the crossover temperature  $T_c$  ( $154 \pm 9$  MeV)<sup>53</sup> of the LQCD calculation. However, for both pressure and energy density high temperature region agrees well with EVHRG model for  $R_h = 0.15$  fm which indicates that interaction is very important to include in the HRG model especially at the high temperature region. At the low temperature region interaction is also there. However its effect is small. It should be noted that  $R_h = 0.15$  fm gives the best fit of the LQCD data upto  $T = 200$  MeV which is already shown in the Fig. 1. The increase of the hardcore radii of all the hadrons further reduces the ability to reproduce both the LQCD results of normalized pressure and normalized energy density as can be seen from the Fig. 2. It is found in Ref.<sup>42</sup> that the equation of state can also be described well with baryonic radius  $0.3 - 0.6$  fm assuming mesons to be point like. In Ref.<sup>28</sup> description of equation of state even higher temperature region ( $T > 200$  MeV) is also improved using a hybrid model of EVHRG and the perturbative QCD. In this work a switching function is used to connect hadronic and the partonic phase. The mass dependent hadronic radius is also considered in EVHRG model to study the hadronic yields at LHC energy and good agreement between model and experimental data is found.<sup>55</sup>

Figure 3 shows the variation of normalized entropy density with the temperature at  $\mu = 0$ . Similar to Fig. 2, results of  $s/T^3$  calculated in the EVHRG model with  $R_h = 0.15$  fm are very close to the LQCD data. For larger radii  $s/T^3$  of EVHRG model under estimate the LQCD results.

### 3.2. Specific heat at $\mu = 0$

The specific heat at constant volume  $C_V$  is given by<sup>53</sup>

$$C_V = \left( \frac{\partial \varepsilon}{\partial T} \right)_V. \quad (16)$$

The  $C_V$  is a sensitive indicator of the transition from hadronic matter to the QGP. The  $C_V$  increases rapidly or even diverges near the transition temperature for a conventional second order phase transition. Although results of pressure, energy



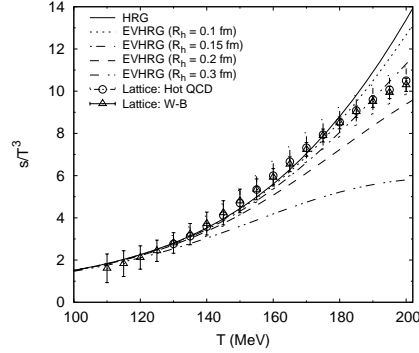


Fig. 3. The variation of normalized entropy density with the temperature at  $\mu = 0$ . Continuum limit lattice QCD data are taken from Hot QCD Collaboration<sup>53</sup> and Wuppertal-Budapest Collaboration<sup>54</sup>

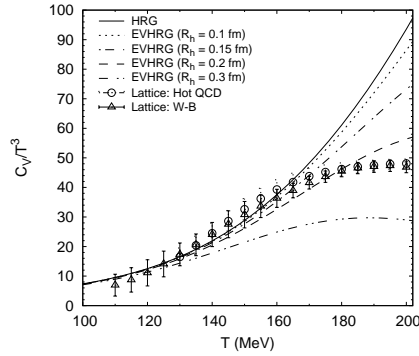


Fig. 4. Variation of normalized specific heat at constant volume with temperature at  $\mu = 0$ . Lattice QCD data for continuum extrapolation are taken from Bazavov *et al.*<sup>53</sup> and Borsanyi *et al.*<sup>54</sup>

density and entropy density in EVHRG model are known already from published literature, result of  $C_V$  in EVHRG model is shown first time in this paper.

Figure 4 shows the temperature dependence of normalized specific heat at  $\mu = 0$ . Similar like normalized pressure and energy density, normalized specific heat calculated in ideal HRG model is very close to the continuum limit LQCD data<sup>53,54</sup> up to the temperature  $T \simeq T_c$ . Results of normalized specific heat calculated in EVHRG model has also been shown in this figure. Normalized specific heat in EVHRG model is suppressed compared to ideal HRG model and the suppression increases with increasing temperature as well as with increasing radii of hadrons because of the repulsive interaction between hadrons. The  $C_V/T^3$  calculated in the

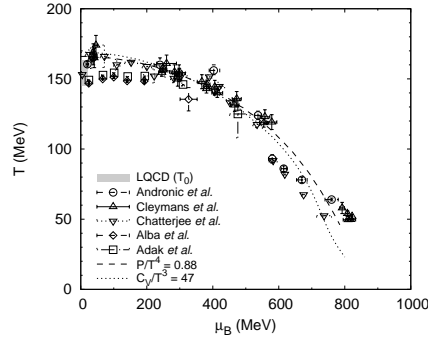


Fig. 5. Chemical freeze-out parameters  $(T, \mu_B)$  obtained by different groups <sup>16,32,35,39,48</sup> at various  $\sqrt{s_{NN}}$  along with the line of  $P/T^4 = 0.88$  and  $C_V/T^3 = 47$  calculated in the ideal HRG model. The blue box shows the uncertainty in LQCD transition temperature ( $154 \pm 9$  MeV) at  $\mu = 0$ .<sup>56</sup>

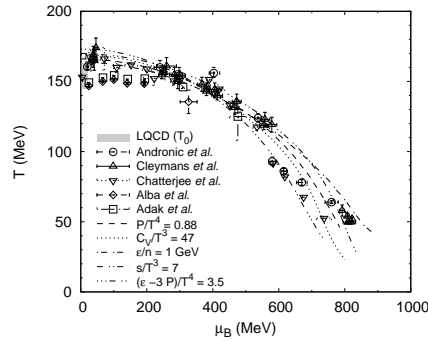


Fig. 6. Same as Fig. 5 but with additional comparisons with other constant chemical freeze-out lines calculated in the ideal HRG model.

EVHRG model with  $R_h = 0.15$  fm is very close to the LQCD data upto  $T = 170$  MeV. For  $R_h = 0.3$  fm  $C_V/T^3$  of EVHRG model matches only qualitatively with LQCD data but not quantitatively.

So from Fig. 2 - 4, it has been observed that results of EVHRG model are close to ideal HRG model only at low temperature region. The effect of interaction is not avoidable at high temperature region. However, to avoid complicity the modeling of the HRG as the ideal gas was considered in most of the works.

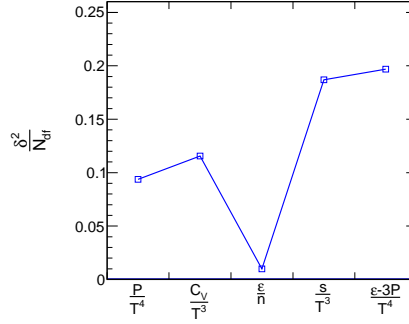


Fig. 7. The deviation,  $\delta^2$  per degrees of freedom for different observables related to the universal chemical freeze out lines shown in Fig. 6.

### 3.3. $P/T^4$ and $C_V/T^3$ at chemical freeze-out

The thermal fireball created due to heavy ion collision expands and cools. At the initial stage, a large number of particles are produced due to deposition of a huge amount of energy in the core of the collision. At this stage, particles collide mostly inelastically. After some time inelastic collisions among the particles stop and hence hadronic yields or ratios get fixed. This stage is called chemical freeze-out. It is already mentioned in the Sec. 1 that, from the experimental information about hadronic ratios or hadronic yields chemical freeze-out parameters can be calculated phenomenologically<sup>15,16,35–39</sup>. Although, all those calculations ignored any dynamics of the system. Chemical freeze-out parameters can also be calculated phenomenologically from experimental data of fluctuations<sup>32,48</sup>. There are several universal chemical freeze-out descriptions in the existing literature which give quite satisfactory descriptions of the hadronic multiplicities measured in heavy-ion collisions. These universal chemical freeze-out properties include  $\epsilon/n = 1$  GeV<sup>35,57</sup>,  $s/T^3 = 7$ <sup>58</sup>,  $n_B + n_{\bar{B}} = 0.12$  fm<sup>-3</sup><sup>59</sup>,  $(\epsilon - 3P)/T^4 = 7/2$ <sup>22</sup> etc., where  $n_B$  is the baryon density and  $n_{\bar{B}}$  is the anti-baryon density. In this paper, two more universal descriptions of chemical freeze-out have been proposed, namely  $P/T^4 \simeq 0.88$  and  $C_V/T^3 \simeq 47$ .

Figure 5 shows chemical freeze-out parameters in  $(T, \mu_B)$  plane calculated in HRG model by different groups<sup>16,32,35,39,48</sup> along with  $P/T^4 = 0.88$  and  $C_V/T^3 \simeq 47$  calculated in the ideal HRG model. Different symbols with error bars represent phenomenologically calculated chemical freeze-out parameters from experimental data at different  $\sqrt{s_{NN}}$  ranging from a couple of GeV at SIS up to several TeV at LHC. In the Fig. 5 dashed line shows  $P/T^4 = 0.88$  whereas dot line shows  $C_V/T^3 = 47$ . It can be seen that this constant normalized pressure can reproduce chemical freeze-out parameters at various  $\sqrt{s_{NN}}$  in  $(T, \mu_B)$  plane. Similarly,  $C_V/T^3 = 47$  calculated in the ideal HRG model reproduces very well the chemical freeze-out

diagram. The blue box in this figure shows the uncertainty in LQCD transition temperature ( $T_0 = 154 \pm 9$  MeV)<sup>56</sup> at  $\mu = 0$ . The  $P/T^4 = 0.88$  and  $C_V/T^3 = 47$  lines touch the temperature axis at slightly higher temperatures than  $T_0$ .

Figure 6 is same as Fig. 5 but with additional comparisons with other constant chemical freeze-out lines calculated in the ideal HRG model. It can be seen that the present work is consistent with the previous works related to universal chemical freeze-out descriptions<sup>22,35,45,57,58</sup>. It is worth mentioning that the conservation laws given in Eqs. 7- 8 have been incorporated during calculations of different observables in  $(T, \mu_B)$  plane.

To show the goodness of theoretical curves, a quantity is defined as:

$$\delta^2 = \sum_i \frac{(O_u - O_i)^2}{O_i^2}, \quad (17)$$

where sum is over the chemical freeze-out points,  $O_i$  and  $O_u$  are respectively the values of the observable at the  $i$  th point and its universal (fixed) value described previously. For an example, if  $O_i$  is  $P/T^4(T_i, \mu_i)$  then  $O_u = 0.88$ . Figure 7 shows the deviation,  $\delta^2/N_{df}$  for different observables where  $N_{df}$  is the number of degrees of freedom *i.e.*, the number of point less the number of parameters in the model. It can be seen that  $\varepsilon/n = 1$  GeV gives the best description of the chemical freeze-out parameters. Further, deviations for  $P/T^4 = 0.88$  and  $C_V/T^3 = 47$  are less compared to that of  $s/T^3 = 7$  and  $(\varepsilon - 3P)/T^4 = 3.5$ .

Let us now discuss the physical interpretation of the proposed universal chemical freeze-out lines. It is really remarkable to see that some basis thermodynamic quantities do not change along the chemical freeze-out line over a large energy range. This indicates the equilibration of the thermal matter even at lower collision energy. In the Boltzmann approximation,  $P/T^4$  and  $C_V/T^3$  can be written as

$$\frac{P}{T^4} = \sum_i \frac{g_i z_i m_i^2}{2\pi^2 T^2} K_2\left(\frac{m_i}{T}\right), \quad (18)$$

$$\frac{C_V}{T^3} = \sum_i \frac{g_i z_i}{2\pi^2} \left( 12 \frac{m_i^2}{T^2} K_2\left(\frac{m_i}{T}\right) + \frac{m_i^4}{T^4} K_2\left(\frac{m_i}{T}\right) + 3 \frac{m_i^3}{T^3} K_1\left(\frac{m_i}{T}\right) \right). \quad (19)$$

where  $z_i = \exp(\mu_i/T)$  is the fugacity for the  $i$  th hadron. At very high energy collision (say LHC energy) chemical freeze-out  $T$  does not vary much with the change of  $\sqrt{s_{NN}}$  and  $z_i \sim 1$  since  $\mu_i$  becomes almost zero. Hence  $P/T^4$  and  $C_V/T^3$  remain fixed. At low energy the  $P/T^4$  is effected by two factors;  $z_i/T^2$  and the  $K_2(1/T)$  for a fixed  $m_i$ . With the decrease of collision energy chemical freeze-out  $T$  decrease whereas  $\mu_i$  increases. Therefore  $z_i/T^2$  increases and the other function  $K_2(1/T)$  decreases. As a result,  $P/T^4$  of the hadron gas remains almost constant. Similarly, with the decrease of collision energy each term of  $C_V/T^3$  in Eq. 19 remains almost constant. In the hadronic matter pressure and energy density are related by the equation  $P = c_s^2 \varepsilon$ , where  $c_s^2$  is the speed of sound of the medium. Now the

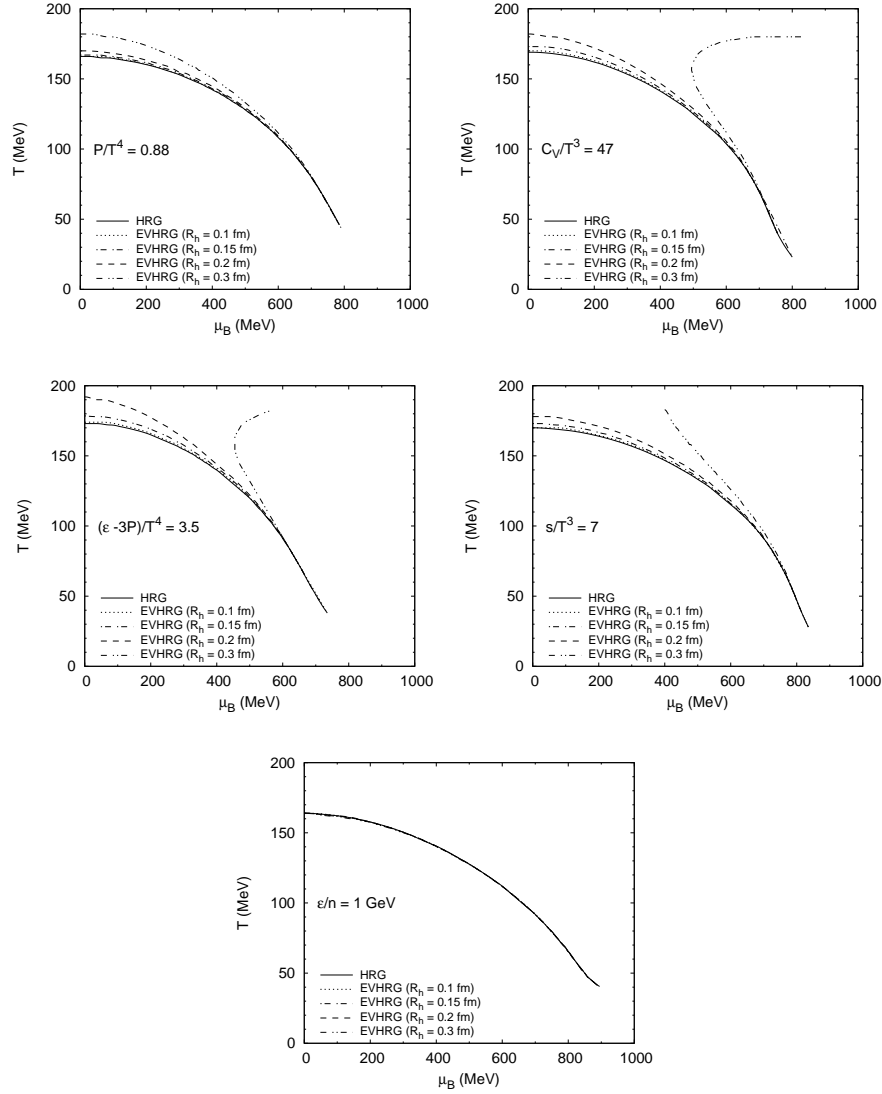


Fig. 8. Variation of universal chemical freeze-out lines with hadronic radii  $R_h$ .

specific heat is related to the  $c_s^2$  by the following equation<sup>53</sup>

$$c_s^2 = \frac{\partial P}{\partial \varepsilon} = \frac{\frac{\partial P}{\partial T}}{\frac{\partial \varepsilon}{\partial T}} = \frac{s}{C_V}. \quad (20)$$

For a massless, noninteracting gas,  $c_s^2 = 1/3$ . For a hadronic medium  $c_s^2$  is expected to be less than that. In Ref.<sup>61</sup> it was shown that the hadronic spectra can be

described well in Landau hydrodynamical model with  $c_s^2 = 0.2$ . In this present work we note that along the chemical freeze-out line  $c_s^2$  is constant and has the value  $\simeq 0.15$  ( $\simeq 7/47$ ) since both  $s/T^3$  and  $C_V/T^3$  are constant along this line. This tells that medium properties in terms of  $c_s^2$  are also similar along the chemical freeze-out line *i.e.*, in all collision energies.

#### 4. Sensitivity of chemical freeze-out lines on repulsive interaction

Repulsive interaction affects the equation of states of the thermal system at high temperature which is already discussed in this paper. Therefore, it is necessary to study the sensitivity of universal chemical freeze-out lines in presence of repulsive interaction.

Figure 8 shows different universal chemical freeze-out conditions in EVHRG model for different radii of hadrons. There is no effect of repulsive interaction is there at chemical freeze-out  $\varepsilon/n = 1$  GeV condition. This is because suppression factor,  $(1 + \sum_k V_{ev,k} n_k^{id}(T, \mu_k))$  is there at the denominator for both energy density and number density as can be seen from the Eqs. 11-13. For all other universal chemical freeze-out conditions effect of repulsive interaction is clearly visible. However, for  $R_h = 0.15$  fm at which  $\chi^2$  is minimum (Fig. 1), universal chemical freeze-out lines deviate from the corresponding lines of ideal HRG only upto 3% but qualitative behaviors remain same. Although at very large radii (say  $R_h = 0.3$  fm, for an example) shapes of the universal chemical freeze-out lines for  $C_V/T^3 = 47$ ,  $(\varepsilon - 3P)/T^4 = 3.5$  and  $s/T^3 = 7$  become different compared to ideal HRG model.

#### 5. Conclusions

I conclude that at high temperature the ideal HRG model is not good enough to describe LQCD data of pressure, energy density, entropy density and specific heat calculated at  $\mu = 0$ . The EVHRG model with hadronic radii of 0.15 fm gives best description of pressure, energy density where the minimum of  $\chi^2$  has been observed. The same hadronic radii can describe LQCD data of  $s/T^3$  upto  $T = 200$  MeV and of  $C_V/T^3$  upto  $T = 170$  MeV. All these results indicate the importance of repulsive interaction present in the EVHRG model. The chemical freeze-out parameters deduced at various  $\sqrt{s_{NN}}$  are well reproducible in the ideal HRG model using the conditions of constant normalized pressure and constant normalized specific heat respectively. It has been observed that both  $P/T^4 = 0.88$  and  $C_V/T^3 = 47$  calculated in ideal HRG model reproduce very well the chemical freeze-out diagram which indicate that the basic thermodynamic properties of the system created in heavy ion collision are almost similar in all collision energies. Since  $s/T^3$  is also constant along the chemical freeze-out curve,  $C_V/T^3 = 47$  corresponds to  $c_s^2 = 0.15$  of the medium. Further, since repulsive interaction is there in the hadronic medium values of  $P/T^4$  and  $C_V/T^3$  at chemical freeze-out become model dependent. However for our best fit value of hadronic radii ( $R_h = 0.15$  fm) qualitative behaviors of  $P/T^4$  and  $C_V/T^3$  remain similar to ideal HRG model. Hence  $P/T^4$  and  $C_V/T^3$

remain constant at chemical freeze-out even in EVHRG model. In this present work pressure, energy density of the matter are used to extract the hadronic radii. Susceptibilities of conserved charges can also be used for the same purpose. This is beyond the scope of the present analysis and will be treated elsewhere. In some very recent papers, van der Waals attractive interaction is also considered in the hadronic model.<sup>62–66</sup> I plan to study the sensitivity of universal chemical freeze-out lines on the attractive interaction in my future work.

### Acknowledgments

I would like to thank Prof. S. K. Ghosh for useful discussions.

### References

1. Y. Aoki, G. Endrodi, Z. Fodor, S. D. Katz and K. K. Szabo, *Nature* **443**, 675 (2006).
2. M. Asakawa and K. Yazaki, *Nucl. Phys. A* **504**, 668 (1989).
3. R. Hagedorn and J. Rafelski, *Phys. Lett.* **97B**, 136 (1980).
4. D. H. Rischke, M. I. Gorenstein, H. Stoecker and W. Greiner, *Z. Phys. C* **51**, 485 (1991).
5. J. Cleymans, M. I. Gorenstein, J. Stalnacke and E. Suhonen, *Phys. Scripta* **48**, 277 (1993).
6. P. Braun-Munzinger, J. Stachel, J. P. Wessels and N. Xu, *Phys. Lett. B* **344**, 43 (1995).
7. J. Cleymans, D. Elliott, H. Satz and R. L. Thews, *Z. Phys. C* **74**, 319 (1997).
8. G. D. Yen, M. I. Gorenstein, W. Greiner and S. N. Yang, *Phys. Rev. C* **56**, 2210 (1997).
9. P. Braun-Munzinger, I. Heppe and J. Stachel, *Phys. Lett. B* **465**, 15 (1999).
10. J. Cleymans and K. Redlich, *Phys. Rev. C* **60**, 054908 (1999).
11. P. Braun-Munzinger, D. Magestro, K. Redlich and J. Stachel, *Phys. Lett. B* **518**, 41 (2001).
12. P. Braun-Munzinger, K. Redlich and J. Stachel, invited review in *Quark Gluon Plasma 3*, eds. R.C. Hwa and X.N. Wang, (World Scientific Publishing, 2004), [nucl-th/0304013].
13. F. Karsch, K. Redlich and A. Tawfik, *Phys. Lett. B* **571**, 67 (2003).
14. A. Tawfik, *Phys. Rev. D* **71**, 054502 (2005).
15. F. Becattini, J. Manninen and M. Gazdzicki, *Phys. Rev. C* **73**, 044905 (2006).
16. A. Andronic, P. Braun-Munzinger and J. Stachel, *Nucl. Phys. A* **772**, 167 (2006).
17. A. Andronic, P. Braun-Munzinger and J. Stachel, *Phys. Lett. B* **673**, 142 (2009) Erratum: [*Phys. Lett. B* **678**, 516 (2009)].
18. V. V. Begun, M. Gazdzicki and M. I. Gorenstein, *Phys. Rev. C* **88**, 024902 (2013).
19. A. Andronic, P. Braun-Munzinger, J. Stachel and M. Winn, *Phys. Lett. B* **718**, 80 (2012).
20. S. K. Tiwari, P. K. Srivastava and C. P. Singh, *Phys. Rev. C* **85**, 014908 (2012).
21. J. Fu, *Phys. Lett. B* **722**, 144 (2013).
22. A. Tawfik, *Phys. Rev. C* **88**, 035203 (2013).
23. P. Garg, D. K. Mishra, P. K. Netrakanti, B. Mohanty, A. K. Mohanty, B. K. Singh and N. Xu, *Phys. Lett. B* **726**, 691 (2013).
24. A. Bhattacharyya, S. Das, S. K. Ghosh, R. Ray and S. Samanta, *Phys. Rev. C* **90**, no. 3, 034909 (2014).

25. A. Bhattacharyya, R. Ray, S. Samanta and S. Sur, Phys. Rev. C **91**, 041901 (2015).
26. G. P. Kadam and H. Mishra, Phys. Rev. C **92**, 035203 (2015).
27. G. P. Kadam and H. Mishra, Phys. Rev. C **93**, 025205 (2016).
28. M. Albright, J. Kapusta and C. Young, Phys. Rev. C **90**, 024915 (2014).
29. M. Albright, J. Kapusta and C. Young, Phys. Rev. C **92**, 044904 (2015).
30. A. Bhattacharyya, S. K. Ghosh, R. Ray and S. Samanta, EPL **115**, 62003 (2016).
31. V. Begun, Phys. Rev. C **94**, 054904 (2016).
32. R. P. Adak, S. Das, S. K. Ghosh, R. Ray and S. Samanta, Phys. Rev. C **96**, 014902 (2017).
33. H. j. Xu, Phys. Lett. B **765**, 188 (2017).
34. J. H. Fu, Phys. Rev. C **96**, 034905 (2017).
35. J. Cleymans, H. Oeschler, K. Redlich and S. Wheaton, Phys. Rev. C **73**, 034905 (2006).
36. N. Xu and M. Kaneta, Nucl. Phys. A **698**, 306 (2002).
37. A. Andronic, P. Braun-Munzinger and J. Stachel, Nucl. Phys. A **834**, 237C (2010).
38. F. Karsch and K. Redlich, Phys. Lett. B **695**, 136 (2011).
39. S. Chatterjee, S. Das, L. Kumar, D. Mishra, B. Mohanty, R. Sahoo and N. Sharma, Adv. High Energy Phys. **2015**, 349013 (2015).
40. V. Vovchenko and H. Stcker, J. Phys. G **44**, 055103 (2017).
41. V. Vovchenko and H. Stoecker, Phys. Rev. C **95**, 044904 (2017).
42. L. M. Satarov, V. Vovchenko, P. Alba, M. I. Gorenstein and H. Stoecker, Phys. Rev. C **95**, 024902 (2017).
43. V. Vovchenko, M. I. Gorenstein, L. M. Satarov and H. Stoecker, arXiv:1606.06350 [hep-ph].
44. D. R. Oliinychenko, K. A. Bugaev, V. V. Sagun, A. I. Ivanytskyi, I. P. Yakimenko, E. G. Nikonov, A. V. Taranenko and G. M. Zinovjev, arXiv:1611.07349 [nucl-th].
45. A. Tawfik, M. Y. El-Bakry, D. M. Habashy, M. T. Mohamed and E. Abbas, Int. J. Mod. Phys. E **25**, 1650018 (2016).
46. K. A. Olive *et al.* [Particle Data Group], Chin. Phys. C **38**, 090001 (2014).
47. R. Dashen, S. K. Ma and H. J. Bernstein, Phys. Rev. **187**, 345 (1969).
48. P. Alba, W. Alberico, R. Bellwied, M. Bluhm, V. Mantovani Sarti, M. Nahrgang and C. Ratti, Phys. Lett. B **738**, 305 (2014).
49. V. Vovchenko, D. V. Anchishkin and M. I. Gorenstein, Phys. Rev. C **91**, 024905 (2015).
50. J. Kapusta, M. Albright and C. Young, Eur. Phys. J. A **52**, 250 (2016).
51. A. Andronic, P. Braun-Munzinger, K. Redlich and J. Stachel, J. Phys. Conf. Ser. **779**, no. 1, 012012 (2017).
52. P. Alba, W. M. Alberico, A. Nada, M. Panero and H. Stcker, Phys. Rev. D **95**, 094511 (2017).
53. A. Bazavov *et al.* [HotQCD Collaboration], Phys. Rev. D **90**, 094503 (2014).
54. S. Borsanyi, Z. Fodor, C. Hoelbling, S. D. Katz, S. Krieg and K. K. Szabo, Phys. Lett. B **730**, 99 (2014).
55. P. Alba, V. Vovchenko, M. I. Gorenstein and H. Stoecker, arXiv:1606.06542 [hep-ph].
56. A. Bazavov *et al.*, Phys. Rev. D **85**, 054503 (2012).
57. J. Cleymans and K. Redlich, Phys. Rev. Lett. **81**, 5284 (1998).
58. A. Tawfik, J. Phys. G **31**, S1105 (2005).
59. P. Braun-Munzinger and J. Stachel, J. Phys. G **28**, 1971 (2002).
60. B. Muller, Lect. Notes Phys. **225**, 1 (1985).
61. B. Mohanty and J. e. Alam, Phys. Rev. C **68**, 064903 (2003).
62. V. Vovchenko, D. V. Anchishkin and M. I. Gorenstein, J. Phys. A **48**, 305001 (2015).



63. V. Vovchenko, D. V. Anchishkin and M. I. Gorenstein, Phys. Rev. C **91**, 064314 (2015).
64. V. Vovchenko, D. V. Anchishkin, M. I. Gorenstein and R. V. Poberezhnyuk, Phys. Rev. C **92**, 054901 (2015).
65. K. Redlich and K. Zalewski, Acta Phys. Polon. B **47**, 1943 (2016).
66. V. Vovchenko, M. I. Gorenstein and H. Stoecker, Phys. Rev. Lett. **118**, 182301 (2017).